

N74-14590

FINITE ELEMENT  
STRESS ANALYSIS OF POLYMERS  
AT HIGH STRAINS

by Michel Durand and Etienne Jankovich

KLEBER COLOMBES, Theoretical Tire Engineering,  
COLOMBES, France

SUMMARY

A numerical analysis is presented for the problem of a flat rectangular rubber membrane with a circular rigid inclusion undergoing high strains due to the action of an axial load. The neo-hookean constitutive equations are introduced into the general purpose TITUS program by means of equivalent hookean constants and initial strains. The convergence is achieved after a few iterations. The method is not limited to any specific program. The results are in good agreement with those of a Company sponsored photoelastic stress analysis. The theoretical and experimental deformed shapes also agree very closely with one another. For high strains it is demonstrated that using the conventional HOOKE law the stress concentration factor obtained is unreliable in the case of rubberlike material.

INTRODUCTION

The structure of a radial motor vehicle tire is made up of two types of components namely the reinforcing cords and the rubber. The most immediate problem in tire stress analysis is that of the large displacements in the inflated tire described in a previous paper (Reference 1). It appears that the more important components are the reinforcing cords allowing the tire to take a stable inflated shape. This particular problem can now be considered as solved.

However, in order to solve the complete problem, the rubber's behavior must also be adequately analyzed by means of an as economical as possible modification of existing programs. Up until now, this very challenging problem of non linear material behavior and incompressibility has only been solved in a few special cases (Reference 2).

The aim of the present work is to stress analyze the rubber parts of the tire by using NASTRAN and TITUS. A test specimen encompassing a rigid inclusion is

calculated in uniaxial extension and the results are compared with those of photoelasticity. The experimental evidence shows the limits of validity of these methods now available to the designer.

#### SYMBOLS

(k)	Stiffness matrix, Nm
(B)	Matrix relating strain to nodal displacements, mm/mm
$\Delta$	Surface of the membrane element, m <sup>2</sup>
(D)	Constitutive law in matrix form, Nm <sup>-2</sup>
$\sigma$	Stress, Nm <sup>-2</sup>
$\epsilon$	Strain, mm/mm
$\epsilon_0$	Initial strain, mm/mm
$\nu$	POISSON's ratio, (no units)
W	Elastic potential per unit volume of the unstrained body, Nm <sup>-2</sup>
C <sub>1</sub> and C <sub>2</sub>	Constants of MOONEY, Nm <sup>-2</sup>
I <sub>i</sub>	Strain invariants, i = 1, 2 and 3, (no units)
(E)	Neo-hookean constitutive law of a membrane in matrix form, Nm <sup>-2</sup>
$\sigma_0$	Initial hydrostatic stress of a rubber membrane, Nm <sup>-2</sup>
u	Displacement, m
$\sigma_1$ and $\sigma_2$	Principal stresses in the middle plane of the membrane, Nm <sup>-2</sup>
$\rho$	Radius of curvature of the transverse isostatic, m
s	Curvilinear abscissa, m
$\sigma_0$	Normal stress tangent to the edge of the disc, Nm <sup>-2</sup>
C	Photoelastic material constant, N <sup>-1</sup> m <sup>2</sup>
a	Radius of the disc, m

#### Subscripts:

T	transposed
t	true
x	coordinate perpendicular to the load axis centered in the middle of the inclusion
y	coordinate along the load axis centered in the middle of the inclusion

## GENERAL APPROACH

### HOOKE'S LAW

The elementary tests carried out show that for the material under consideration HOOKE'S law applies in relating true stress \* to strain even in the 35 % mm/mm range. Thus, it may be assumed tentatively that the non linearity of the rubber's constitutive law is only the result of the large displacements experienced by the rubber.

#### Stiffness matrix

The stiffness matrix of the membrane plate element used can be written (Reference 3) :

$$(k) = (B^T) \times (D) \times (B) \times \Delta \times d$$

- d Thickness, m
- $\Delta$  Surface of the membrane element, m<sup>2</sup>
- (B) Matrix relating strain to displacement, mm/mm
- (D) Constitutive law, Nm<sup>-2</sup>

As a result of the incompressibility condition  $\Delta d = \text{const.}$  The accuracy of the forces and the displacements depends on the accuracy of the terms B and D.

#### Definition of D

$$\left\{ \sigma \right\} = [D] \left( \left\{ \begin{array}{c} \epsilon_x \\ \epsilon_y \\ \epsilon_{xy} \end{array} \right\} - \left\{ \epsilon_0 \right\} \right)$$

Experimentally the uniaxial law is

$$\sigma_t = E \epsilon \quad \text{where } E \text{ is YOUNG'S modulus}$$

As a result  $\sigma$  must be replaced by  $\sigma_t$  in the equations. The only remaining term that has to be calculated in the course of the extension of the specimen is B. Thus, this problem would seem to be identical to that of the large displacement problem.

- 
- \* The true stress is computed per unit section area of the deformed body whereas the conventional stress is computed per unit section area of the undeformed body.

In the case of rubber, however, it is well known that there is an additional, pressure type, term "p" in the constitutive equation. To eliminate "p", represented by  $\{D\} \{\epsilon_o\}$  above, an additional equation in terms of displacements must be written for each element. NASTRAN with its scalar element can handle such an equation. The resulting data input problem is however very cumbersome. Thus, this solution may be uneconomical for every day use.

In order to demonstrate the existence of "p" a large displacement calculation was carried out with  $\epsilon_o = 0$  and  $\nu = .5$ . The largest transverse displacement along the x-axis passing through the middle of the inclusion was 13 % in error relative to the experimental values. This error was much larger than the one obtained by means of the theory developed below.

#### MOONEY-RIVLIN CONSTITUTIVE LAW

The most common type of rubber material behavior equation is that of Mooney-Rivlin (Reference 4). Considering that W is the elastic potential measured per unit volume of the unstrained body the postulated function is

$$W = C_1 (I_1 - 3) + C_2 (I_2 - 3)$$

$I_i$  are the strain invariants ( $i = 1, 2$ )

$C_1, C_2$  are the constants postulated by Mooney.

The theory of plane stress of very thin membranes applies to the rubber specimen considered here. The deformations are symmetric about the middle plane of the body and are essentially uniform throughout the thickness. The pressure type component "p" is eliminated because in the present problem the normal stress perpendicular to the specimen's surface is zero. Large displacement equations are used in the B matrix.

The equations obtained are:  $\{\sigma\} = \{E\} \{\epsilon\} + \{\sigma_o\}$

$\sigma$  are defined at points in the deformed body, but are measured per unit area of the undeformed body.

The E and  $\sigma_o$  are functions of not only  $C_1$  and  $C_2$  but also of  $\epsilon_{xx}, \epsilon_{yy}$  and  $\epsilon_{xy}$ . The matrix E is positive definite in the strain range considered.

In uniaxial extension the above equations in terms of true stresses must be identical to the well known equation (Reference 5) :

$$\sigma_t'' = 2 \left( C_1 + \frac{C_2}{\lambda_{11}} \right) \left( \lambda_{11} - \frac{1}{\lambda_{11}^2} \right) \frac{1}{1 - \nu^2} \quad \text{where } \nu = .5$$

and  $\lambda_{11} = 1 + \epsilon_{11}$

This happens only if  $C_2$  is zero and the deformations are limited in size. Such a material is called neo-hookean. The constant  $C_1$  is determined by means of the latter equations in an uniaxial elementary extension test.  $C_1 = .71 \text{ MN m}^{-2}$ .

The solution of the equations is carried out by using an equivalent secant modulus method. The full load is applied in this trial and error approach. The first solution is obtained by the hookean constitutive law where  $\sigma_0$  is set at zero.

#### NASTRAN AND TITUS ANALYSIS

The program of J.T.Oden, OK1, (Reference 6), is designed for analyzing rubberlike material. Thus it came under consideration first, but it can only analyze plane strain plates whereas our problem is a plane stress problem \*.

The solutions obtained by the TITUS and NASTRAN programs have been compared at the first iteration. TITUS uses isoparametric quadrilateral membrane elements while NASTRAN has constant stress CQDMEM elements. The stresses differ only by 2 %. However the difference between the displacements of NASTRAN as compared to those of TITUS was 4 %. The results of NASTRAN were much further away from the experimental ones than those of TITUS. In this particular case the CPU computation time was 50 s for TITUS and 84 s for NASTRAN using UNIVAC 1108 (EXEC 8).

#### MODIFICATION OF TITUS

The TITUS program was developed in France by CITRA now called SPIEBATI-GNOLLES Inc. Because of the proximity of the development team it was easy to modify the program. By means of a minor modification it is possible to calculate the modulus  $E$  and  $\sigma_0$  internally elementwise at each iteration with the help of  $C_1$  and the strains.

The test of convergence was carried out by comparing the arithmetic mean of the displacements obtained at each iteration. At lower loads (9.8 - 19.6 N) the convergence was achieved after about six iterations whereas at 29.4 N ten iterations were needed. In the first case the computation time was 84 s CPU on UNIVAC 1108 (Exec 8).

#### MODELING OF THE PLATE

The finite element idealization of the membrane encompasses 107 nodal points and 84 quadrilateral elements. In order that the theoretical solution and experimental results could be satisfactorily compared, the three loading

---

\* In linear elasticity plane strain and plane stress problems are conjugate. This is not the case, however, for rubberlike materials.

conditions were given in terms of displacements at the end of the specimen. The modeling of the membrane is shown in Fig. 1.

#### Boundary conditions

	Case 1	Case 2	Case 3
Upper line	$u_y = 3.45 \text{ mm}$ $u_x = 0$	$u_y = 6.613 \text{ mm}$ $u_x = 0$	$u_y = 11.79 \text{ mm}$ $u_x = 0$
Around inclusion	$u_y = 0$ $u_x = 0$	$u_y = 0$ $u_x = 0$	$u_y = 0$ $u_x = 0$
Along Y-Axis	$u_x = 0$	$u_x = 0$	$u_x = 0$
Along X-Axis	$u_y = 0$	$u_y = 0$	$u_y = 0$

Since the loading and the deformations are assumed to be symmetrical, only one-quarter of the plate needed to be considered.

#### EXPERIMENTAL WORK

##### TEST SPECIMEN

The model test specimen is a rectangular coupon cut out of a polyurethane plate furnished by PHOTOLASTIC Inc. The coupon is transparent and isotropic when not loaded. A circular hole is cut out of its center and is filled in with araldite which is reinforced with glass beads at a ratio of 100%. The stresses due to the contraction of the disc during polymerisation have been observed by means of crossed polarisors and have been eliminated by an applied compression load in order to keep the neutral state of stress in the specimen. The disc is much stiffer than the rest of the coupon and there is perfect adhesion between them. The grips are glued on to the ends of the rectangle. The only load applied is a vertical load along the specimen's axis and it is measured by means of strain gages. Viscoelastic effects are suppressed by loading up gradually.

The dimensions of the specimen are 117 mm x 42 mm x 1.02 mm and the diameter of the disc is 14 mm.

Using a transmission polariscope, the isoclines are determined with the help of in-plane polarized white light and the isochromes with the help of monochromatic circularly polarized light ( $\lambda_{Na} = 5890 \text{ \AA}$ ).

The isostatics are obtained from the isoclines using graphical means.

### PHOTOELASTIC STRESS ANALYSIS

In rubber the lightwave path difference is proportional to the difference of the principal stresses  $\sigma_1 - \sigma_2$  and also proportional to the instantaneous thickness of the specimen (Reference 7)

$$\delta = C e (\sigma_1 - \sigma_2)$$

The material constant  $C$  is determined by a uniaxial elementary tension test. The value obtained is

$$C = 3.21 \pm 0.03 \text{ m}^2 \text{ daN}^{-1}$$

The principal stresses along the vertical and horizontal symmetry axes are determined by integrating graphically the equation of Lamé and Maxwell (Reference 8)

$$\frac{\sigma_1 - \sigma_2}{\rho_1} + \frac{\partial \sigma_1}{\partial s_1} = 0$$

$$\frac{\sigma_1 - \sigma_2}{\rho_2} + \frac{\partial \sigma_2}{\partial s_2} = 0$$

where  $\rho$  is the radius of curvature of the transverse isostatic and  $s$  is the curvilinear abscissa at a given point. The subscripts 1 and 2 refer to the two families of isostatics.

The starting point of the integration along the x-axis is taken at the edge of the specimen where the stress  $\sigma_2$  is zero.

For the integration along the vertical axis the point of reference for the integration is taken in the region of uniform stress between the grips and the disc where  $\sigma_2$  is zero. Along the edge of the disc the stresses  $\sigma_1$  and  $\sigma_2$  are obtained using the normal stress  $\sigma_\theta$  tangent to the disc and they vary as follows:

$$\frac{\partial \sigma_\theta}{\partial \theta} = - \frac{\partial \sigma_\theta}{\partial r}$$

and 
$$\sigma_1 = \sigma_\theta + (\sigma_1 - \sigma_2) \sin^2 \alpha$$

where  $\alpha$  is the angle between the direction of  $\theta$  and the isostatic  $\sigma_1$ .

The value of  $\sigma_\theta$  is a function of the accuracy of the measurement of the isoclines. As the experimental determination of the latter is relatively inaccurate, in particular at the top of the disc, the accumulated errors may be quite

large. For this reason, starting from the horizontal axis, the values of  $\sigma_1$  and  $\sigma_2$  at the top are 15 % greater than the ones obtained starting from the other axis.

## DISCUSSION OF THE EXPERIMENTAL AND THEORETICAL RESULTS

### DEFORMED SHAPE

The theoretical and experimental results obtained for the deformed shape are in excellent agreement as shown (Figs. 2-4). By different experimental methods the overall transverse displacements at the horizontal symmetry line have been determined as follows:

LOADING	EXPERIMENT	TITUS
	$U_x$ (mm)	$U_x$ (mm)
6 %	- 0.4 ± 0.05	- 0.434
11.5 %	- 0.75 ± 0.05	- 0.806
20.5 %	- 1.4 ± 0.05	- 1.44

### ISOSTATICS

The theoretical and experimental results showing the distribution of the isostatics over the surface of the rubber coupon are plotted in Fig.5. On the left side are shown the calculated principal stresses and on the right side the envelopes of the corresponding experimental principal stresses. Taking into account the fact that the theoretical results are relative to the undeformed surface of the specimen, the agreement is again excellent. The following table shows the values of the applied longitudinal force.

LOADING	EXPERIMENT	TITUS
	Force (N)	Force (N)
6 %	9.8 ± 0.2	10.6
11.5 %	19.6 ± 0.4	18.4
20.5 %	29.4 ± 0.6	28.2

The mesh used in modeling the ends of the specimen was very coarse, the principal aim being to demonstrate the behavior of an inclusion imbedded in a rubber matrix. Thus, the error obtained is accordingly larger in this region.

## ISOCHROMES

The experimental stress distribution over the surface of the specimens has been established by means of the isochromes. No quantitative comparison is shown here as the numerical results are relative to the undeformed shape and are in terms of the conventional stresses, (Fig. 6-8). The automatic plotting of the required true stress isochromes is being developed at the present time.

However, the shape of the isochromes shown agrees qualitatively with the experimental ones. As demonstrated below the numerically obtained longitudinal true stress concentration factor is very accurate. Thus it can be conjectured that the agreement must be also quantitative.

## PRINCIPAL MEMBRANE STRESSES

In Fig. 9 the true principal membrane stresses together with the experimental ones are shown. The shape of the two families of curves obtained are identical. However there is a vertical shift of the theoretical ones relative to the experimental ones. The difference is quite small and remains within the limits of the accuracy of the experiment. It must be noted that at the top of the inclusion, on the y-axis, the experimental results differ according to whether the point is approached from the right or the left. The mean of the two values is located very near to the theoretical point.

At the intersection of the x-axis with the contour of the inclusion two nearly identical compression stresses are obtained experimentally. This result agrees with those obtained by theoretical consideration in reference 9. The numerical calculation gives two stresses of opposite sign, however. This is explained by the fact that the stresses are calculated at the center of gravity of the element. In this region C of Fig. 10, the stress gradient is very large. Thus, even though the  $\sigma_1$  stress is positive at  $\frac{x}{a} = 1.07$ , the calculation point, it is negative at  $\frac{x}{a} = 1$ , that is at the experimental recording point. Taking these facts into account the agreement between the finite element results and those of the experiment is very good.

## STRESS CONCENTRATION FACTOR

The stress concentration of the longitudinal principal stress along the y-axis is plotted in Fig. 10. The maximum stress concentration factors are

Experiment	1.28
Finite element results	1.31
Linear classical elasticity	1.54

The agreement between the experiment and the numerical results is excellent. It can be concluded further that the linear elasticity gives unreliable

stress values in the case of rubber for strains reaching 18 % or more.

#### CONCLUSION

The close agreement obtained between theoretical and experimental results demonstrates the validity of the large displacement equations, and of the neo-hookean constitutive law used in the modified TITUS program. However, the use of the derived method is not limited to any specific program. After some minor modifications any geometrically nonlinear finite element program may be applied to the analysis of rubber at relatively high strain.

The importance of using the proposed theory instead of the conventional HOOKE type formulation to design rubber parts is made evident by the fact that, using the conventional theory, the stress concentration factor of the inclusion obtained has an error of about 20 %.

#### ACKNOWLEDGEMENTS

The authors wish to thank MM. J.LÉVÉQUE and J.P.NOTTIN, Kléber-Colombes, Centre d'Etudes et de Recherches, Bezons, for carrying out the experimental verification and M. Christian VOUILLON, TITUS program manager, SPIEBATIGNOLLES Inc., Paris and M. Ngoc Khai PHAN, STAD Inc., Paris, for their collaboration in using TITUS and NASTRAN.

REFERENCES

1. Durand, Michel, and Jankovich, Etienne: Nonapplicability of Linear Finite Element Programs to the Stress Analysis of Tires. NASTRAN: Users' Experiences, NASA TM X-2637, September 11-12, 1972.
2. Oden, J.T.: Finite Elements of Nonlinear Continua. Mc GRAW-HILL BOOK COMPANY, 1972.
3. Zienkiewicz, O.C.: The Finite Element Method in Engineering Science. Mc GRAW-HILL LONDON, 1971.
4. Mooney, M.: A Theory of Large Elastic Deformation. J.Appl.Phys., vol.11, 1940, pp.582-592.
5. Alexander, H.: A Constitutive Relation for Rubber-Like Materials. Int.J. Engng Sci., vol.6, 1968, pp. 549-563.
6. Key, J.E.: User's Manual for Digital Computer Program OK1, Numerical Analysis of finite Axisymmetric Deformations of Incompressible Elastic Solids of Revolution. University of Alabama, Huntsville, Research Institute - UARI Research Report N° 121.
7. Treloar, L.R.G.: The Physics of Rubber Elasticity. Oxford University Press, 1958, pp. 197-234.
8. Le Boiteux, H. and Broussard, R.: Elasticité et Photoelasticimétrie. Herman, Paris, 1940.
9. Rehner, John Jr.: Theory of Filler Reinforcement in Natural and Synthetic Rubber. The Stresses In and About the Particles. Rubber Chemistry and Technology, vol. 17, 1944, pp. 865-874.

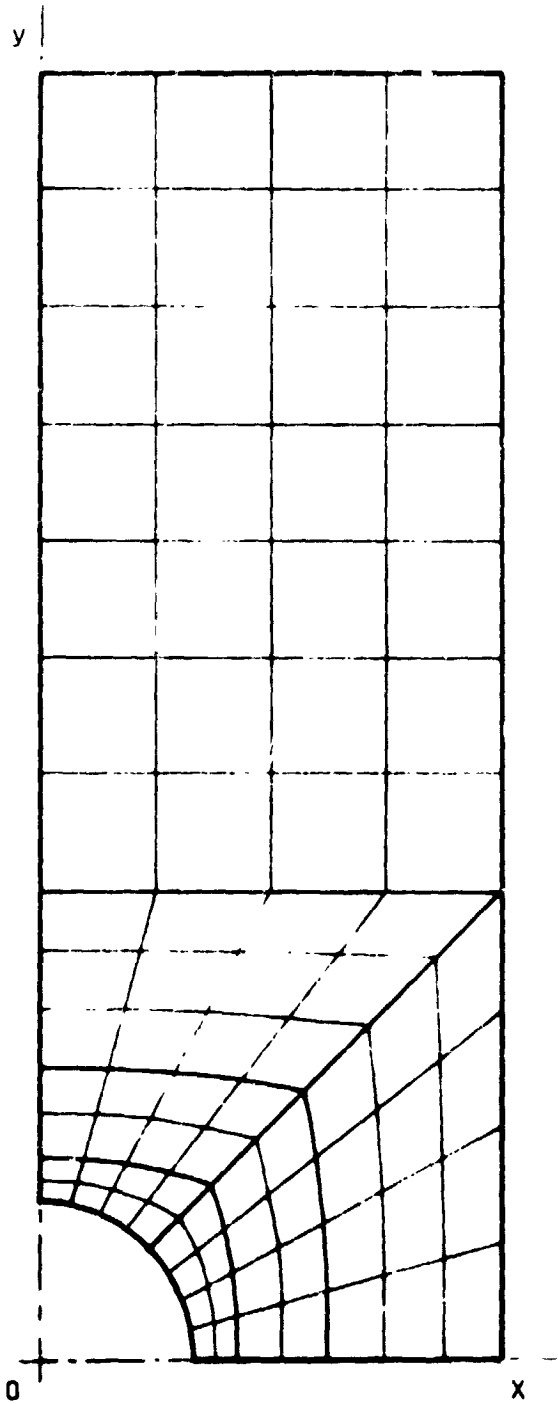
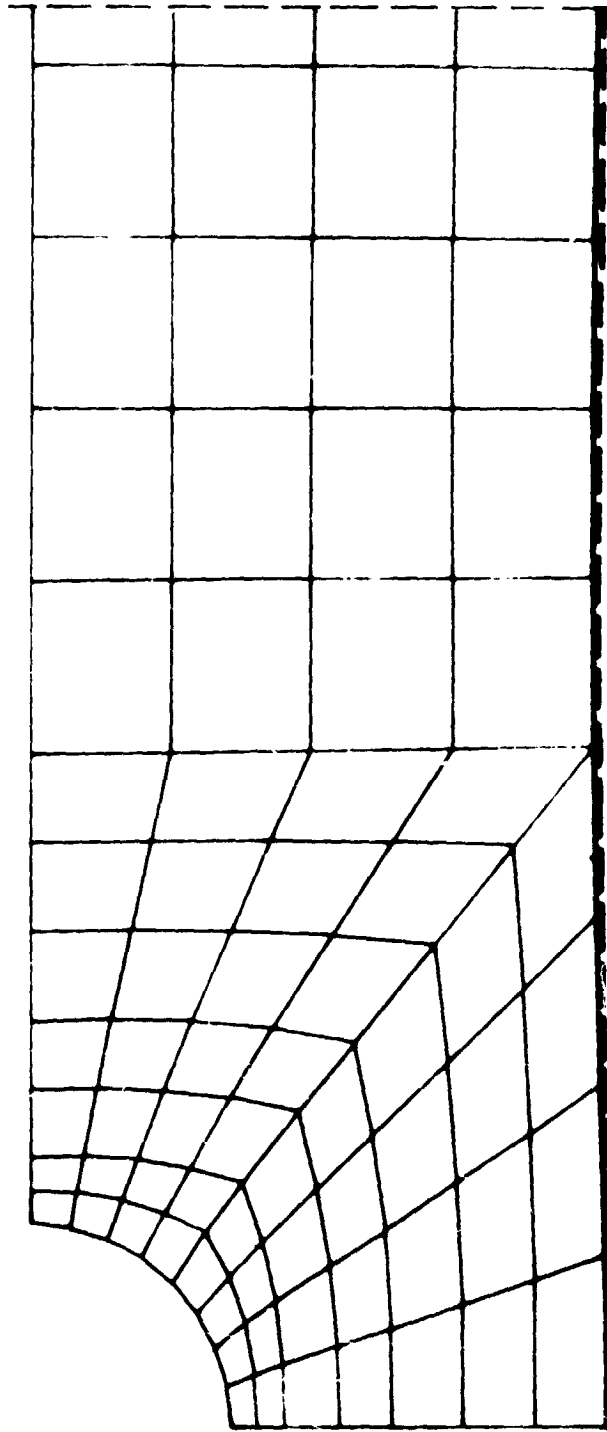
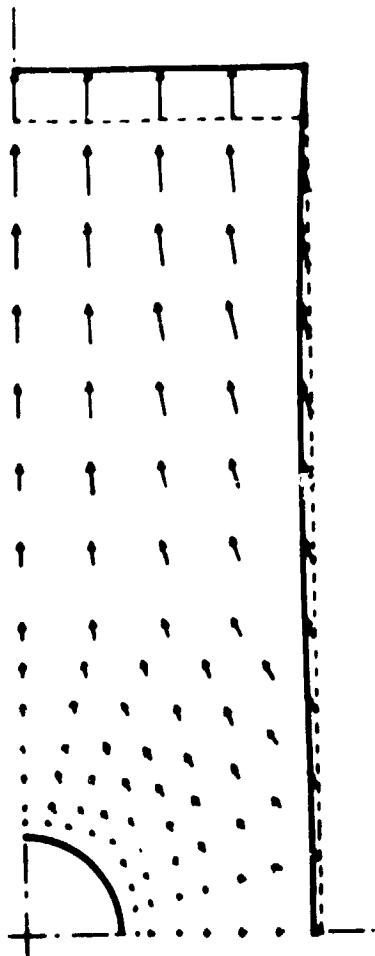


Figure 1. - Super-Elements and Automatically Generated Mesh by TITUS.

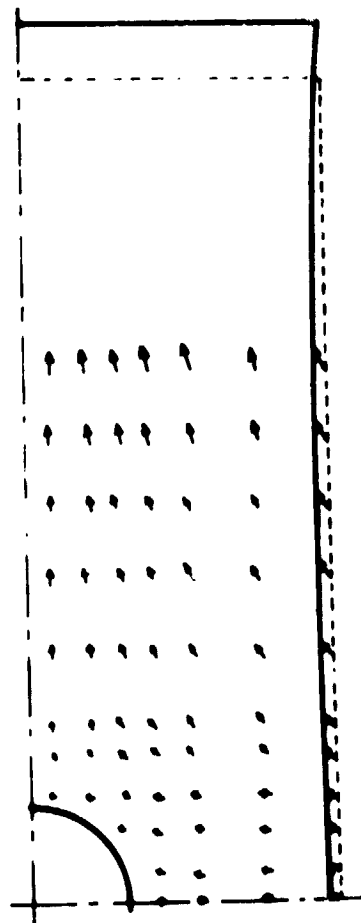


—— TITUS  
- - - Experiment

Figure 2. - Finite Element Solution and Experimental Deformed Shape  
Load = 19.6 Newtons.

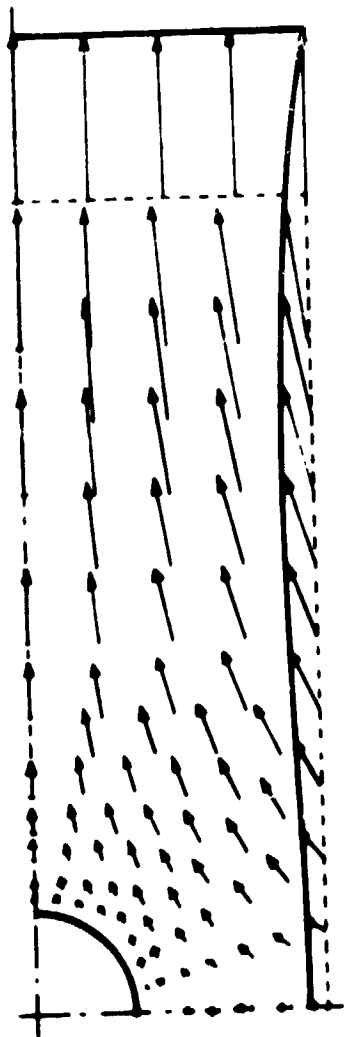


TITUS Solution

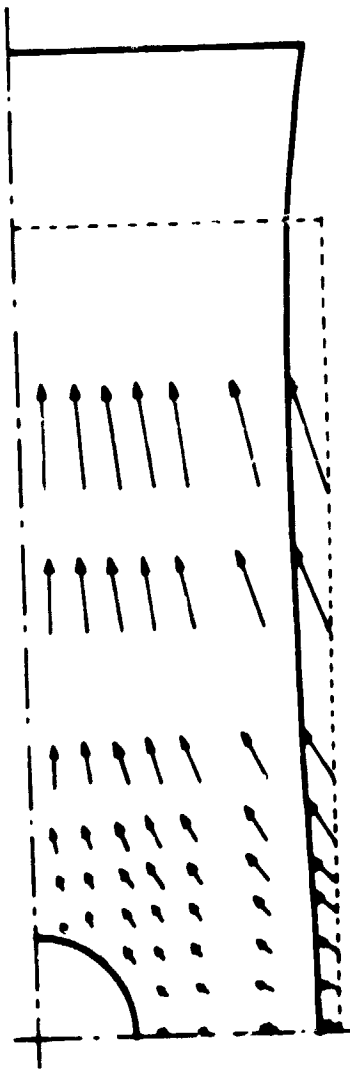


Experiment

Figure 3. - Displacement Vectors. Load = 9.81 Newtons.

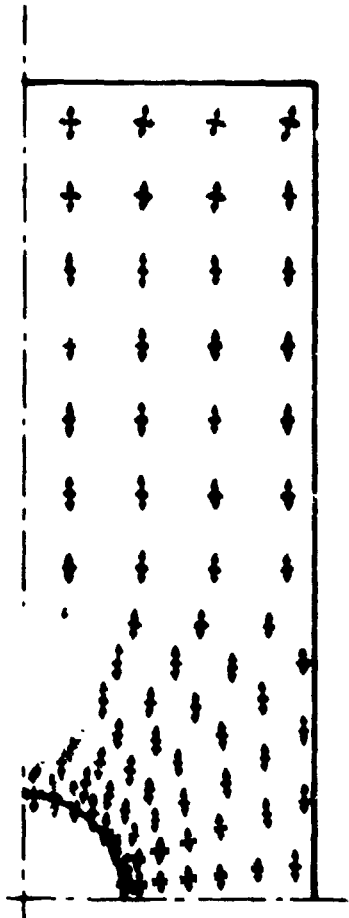


TITUS Solution

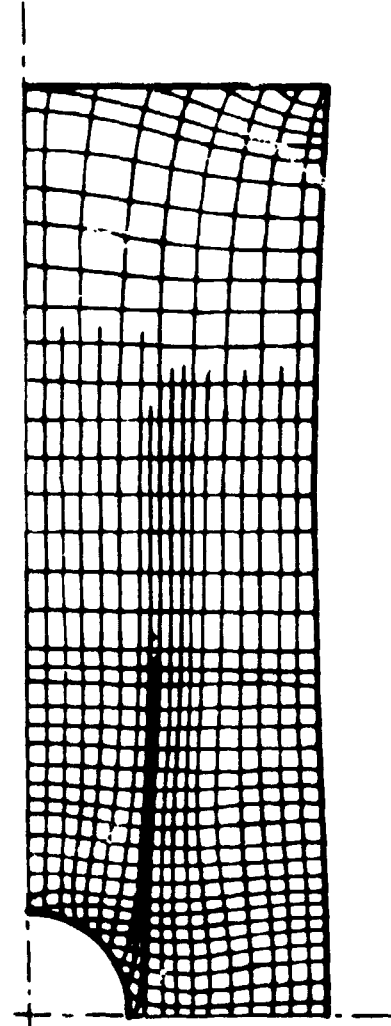


Experiment

Figure 4. - Displacement Vectors. Load = 29.4 Newtons.

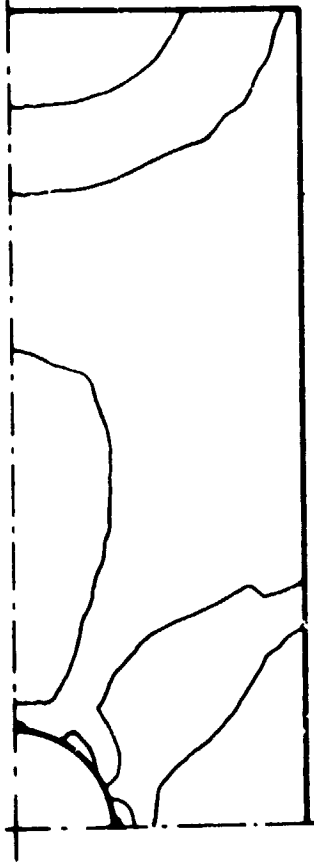


Conventional Principal Stresses  
on the Undeformed Shape  
(TITUS)

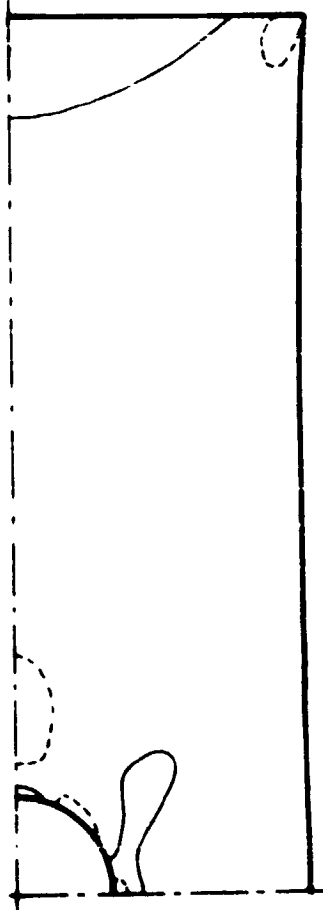


Experimental Isostatics  
- Principal True Stress Envelopes -  
on the Deformed Shape

Figure 5. - Conventional Principal Stresses and Experimental Isostatics.  
Load = 19.6 Newtons.

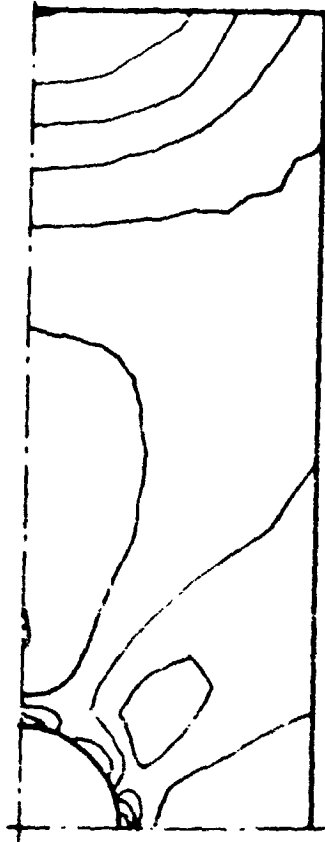


TITUS Solution  
 Difference of the  
 Conventional Principal  
 Membrane Stresses  
 in the Undeformed Body

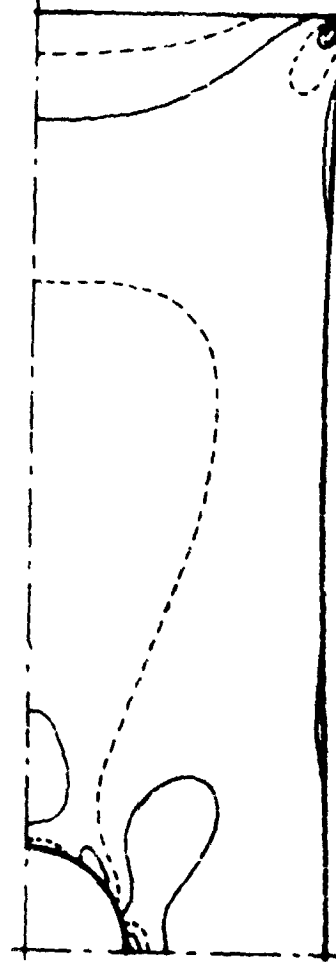


Experiment  
 Isochromes - Difference of the  
 True Principal  
 Membrane Stresses  
 in the Deformed Body

Figure 6. - Isochromes - Numerical Results and Experiment.  
 Load = 3.61 Newtons.

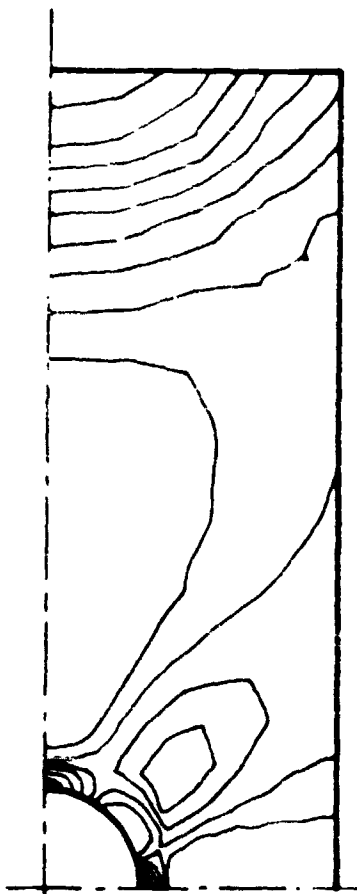


TITUS Solution  
 Difference of the  
 Conventional Principal  
 Membrane Stresses  
 in the Undeformed Body

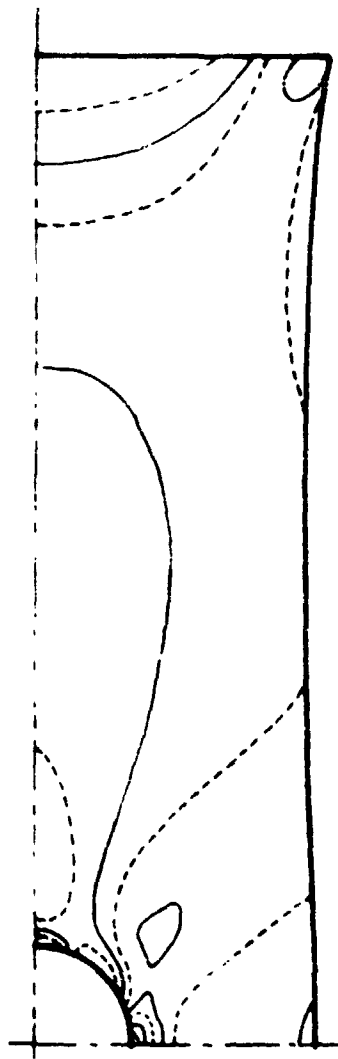


Experiment  
 Isochromes - Difference of the  
 True Principal  
 Membrane Stresses  
 in the Deformed Body

Figure 7. - Isochromes - Numerical Results and Experiment.  
 Load = 19.6 Newtons.



TITUS Solution  
 Difference of the  
 Conventional Principal  
 Membrane Stresses  
 in the Undeformed Body



Experiment  
 Isochromes - Difference of the  
 True Principal  
 Membrane Stresses  
 in the Deformed Body

Figure 8. - Isochromes - Numerical Results and Experiment,  
 Load = 29.4 Newtons.

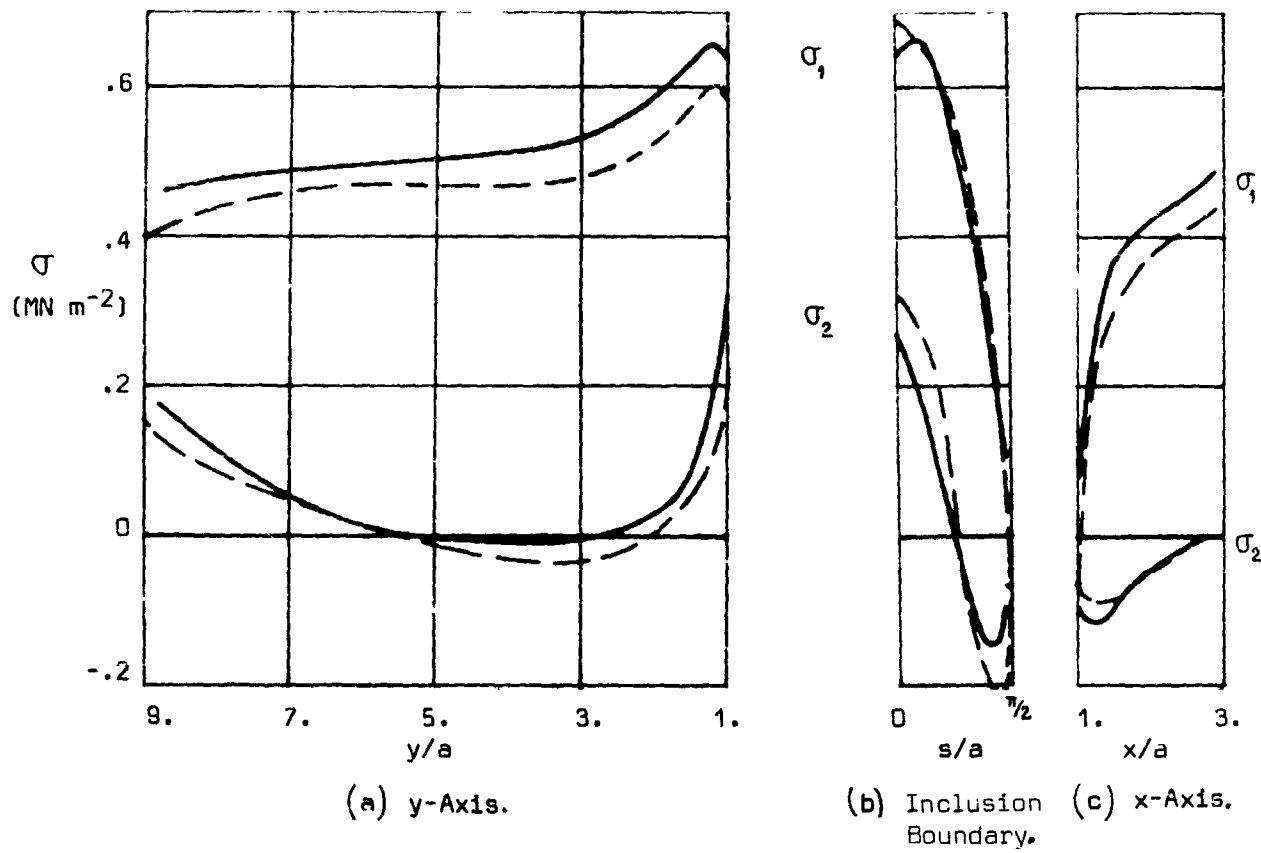


Figure 9. - True Principal Stresses at a Load = 19.6 Newtons.

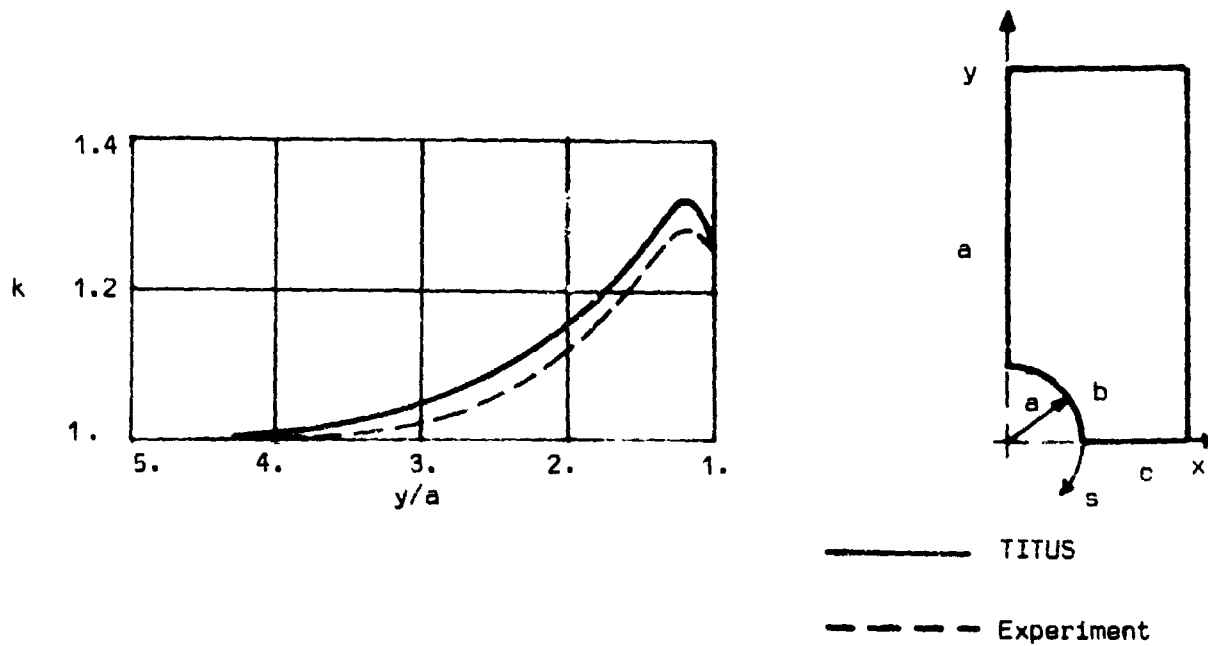


Figure 10. - Longitudinal True Stress Concentration Factor vs. y-Axis. Load = 19.6 Newtons.